Coupled electron and nonequilibrium optical phonon transport in a GaAs quantum well

G. Paulavičius, V. V. Mitin, and N. A. Bannov[a)]
Department of Electrical and Computer Engineering, Wayne State University, Detroit, Michigan 48202

(Received 30 September 1996; accepted for publication 26 August 1997)

The self-consistent Monte Carlo technique has been used to solve coupled nonlinear kinetic equations for electrons and optical phonons confined in a GaAs quantum well. We have studied the influence of nonequilibrium phonons on quasi-two-dimensional electron transport for a lattice temperature of 30 K and for a wide range of applied electric fields. A substantial difference in generation and decay times as well as the confinement inside the GaAs/AlAs heterostructure-bounded active region lead to a significant growth of nonequilibrium optical-phonon population generated by a heated electron gas. We have found that when the phonon generation (as well as phonon reabsorption by the quasi-two-dimensional carriers) becomes significant, there are substantial effects on transport in the quantum well. We show that for low electron concentrations, the hot optical-phonon distribution reflects the main features of the carrier distribution; indeed, it preserves an average quasi-momentum in the forward (opposite to electric field) direction. However, hot-phonon feedback to the electron system is found to be not essential in this case. For high electron concentrations, enhanced nonequilibrium optical-phonon reabsorption results in phonon distribution which spreads significantly in the quasi-momentum space and essentially loses the characteristic of the forward-peaked anisotropy. The interactions with the confined electron subsystem typically result in an isotropic phonon distribution. In this case, nonequilibrium optical phonons lead to an increase in the mean electron energy and a reduction in the carrier drift velocity.
 [S0021-8979(97)01123-7]

I. INTRODUCTION

Modern solid-state electronics is entering a new stage of development with a strong emphasis on utilizing quantum well (QW) semiconductor structures. However, full use of the advantages of QW structures cannot be realized completely without an adequate knowledge of how the coupled electron-phonon system responds to realistic nonequilibrium external conditions. This response becomes much more complex when nonequilibrium (hot) phonon effects come into play and strongly affect all-important electron transport parameters.

In A_3B_5 materials, a substantial difference between optical-phonon emission and their decay characteristic times, τ_0 and τ_d, respectively, may result in a significant accumulation of these phonon modes. In the case of GaAs, $\tau_0 \approx 0.15$ ps and $\tau_d \approx 7-8$ ps. (The latter value is realistic at the low lattice temperatures[1–3] for which we have performed our simulation.) If electrons are heated by an applied electric field, photoexcitation, or due to injection into the active region, the optical-phonon population may grow significantly in comparison with the equilibrium population given by the Planck formula.

The hot phonons created by the heated carrier gas may be observed by Raman spectroscopy measurements.[4] Such experiments on nonequilibrium phonon dynamics in bulk GaAs and wurtzite GaN have been reported in Refs. 3 and 5. The population relaxation time for longitudinal optical (LO) phonons was measured directly to be close to 5.0 ps in GaN at $T = 25$ K. A similar value was obtained for GaAs in the 150–420 K temperature range.[3]

Sub-picosecond laser pulses have also been used to study nonequilibrium electron distributions and to generate hot LO phonons in InP and InAs.[6] Since these two semiconductors have considerably different energy band gaps, they provide a contrast in that the decay of the Raman signal probes different electron relaxation mechanisms in the structures investigated. The study shows that the signal decay in narrow-band gap InAs is governed by intervalley $\Gamma - L$ electron transitions, while in wideband gap InP it is dominated by the relaxation of hot LO phonons.

Hot optical phonons dramatically affect electron transport in small scale A_3B_5 semiconductor structures. In general, an increase in the reabsorption of such emitted phonons by electrons increases the mean carrier energy. This, in turn, raises the electron temperature and, hence, reduces the mobility.[1] However, a strong anisotropy of the nonequilibrium phonon distribution in the applied field direction could also result in momentum transfer from the forward optical-phonon modes to electrons causing mutual carrier-phonon drag effects.[1,2,7,8] The competition of these two opposing mechanisms—hot-phonon drag and diffusive heating by phonons—determines the electron mobility in each particular case. It should be pointed out that hot-LO phonon drag is strongly pronounced in quantum wires.[7] In contrast, due to the existence of additional degrees of freedom in QWs and bulk materials, carrier interactions with randomly oriented optical phonons can outweight the drag effect smearing out the electron distribution function and reducing the carrier mobility. A slight increase in the mobility as a result of pre-

[a)]Current address: Box 7911, ECE, NCSU, Raleigh, NC 27695.

vailing hot-phonon drag may be observed only at low electric field.[1,2] However, the effect is comparably small because of a negligible nonequilibrium optical-phonon population accumulated in the structure in this case.

It was shown that hot-phonon reabsorption is important for high-field electron transport in semiconductor quantum wells and wires, resonant heterostructure tunneling diodes, and other microstructures.[7–11] In particular, it was predicted and demonstrated numerically that the quantum cascade laser's[12] performance suffers from relatively high threshold currents[13] but can be improved significantly by the appropriate use of nonequilibrium-phonon effects in the active QW region.

Hot-phonon effects in bulk semiconductors and microstructures have been investigated by several authors.[3,5,6,14–26] However, in spite of active research on nonequilibrium electrons and phonons in small scale systems, such as GaAs quantum wells, there is no adequate understanding of nonequilibrium carrier relaxation, recombination, and noise when both quantization of carriers and confinement of optical phonon modes become important.[27] Most of the previous research in this area is concentrated basically on the influence of nonequilibrium phonons on the electron energy relaxation after initial electro- or photoexcitation. In addition, there have not been enough studies dedicated to a detailed investigation of quasi-two-dimensional (2D) electron transport under hot-phonon conditions in the case of strong carrier-optical-phonon coupling. Earlier theoretical studies on the influence of hot phonons on the electron mean energy and drift velocity as well as on electron and phonon distribution functions in QWs involve the investigation of specific cases when, e.g., only the lowest energetic subband is populated by electrons, or by the use bulklike optical phonon modes and/or *a priori* specified electron distribution functions, etc. Very few of the previous articles studied how nonequilibrium-phonon effects depend on electron concentration and electric field.

We would like to emphasize that electron transport in QWs in the presence of hot phonons is nonlinear with respect to both the carrier and phonon concentrations. Its investigation requires solving coupled nonlinear kinetic equations for both electron and phonon distribution functions. We have solved these equations self-consistently for a GaAs quantum well for a wide range of applied electric fields, and this article presents the main results of our study. We have examined the nonequilibrium optical-phonon distribution as well as its dependence on the applied electric field and electron concentration; also we have investigated the influence of hot phonons on the nonlinear electronic response in this case.

II. MODEL

We have studied the nonlinear electron and phonon dynamics in a quasi-two-dimensional GaAs QW embedded in an AlAs matrix. The thickness of the well, a, has been chosen to be 100 Å in order to reduce the number of ''active'' electron subbands in the QW (practically only the lowest energy subband is populated in equilibrium) and to diminish the role of electron intersubband transitions. At the same time this keeps the well reasonably wide, so that the interface optical modes are not important.[28,29]

The in-plane dimensions of the QW, $L_x \times L_y$, are large in comparison with the electron de Broglie wavelength. In GaAs/AlAs heterostructures, at the top and bottom boundaries of the plane heterointerfaces, there exist large potential barriers for electrons causing carrier wave confinement in the transverse direction.[30] The presence of the heterointerfaces gives rise to a similar confinement of optical-phonon modes in the GaAs layer as well.[13,27] The parameters of this QW structure are favorable for nonequilibrium phonon accumulation because the lowest order confined optical-phonon mode is the only one which scatters 2D electrons with high efficiency.

We use a standard ensemble Monte Carlo method to solve the coupled nonlinear kinetic equations for electrons and phonons. A multi-subband parabolic electron energy-band structure and electron intersubband/intrasubband scatterings by optical and acoustic phonons are taken into account. (However, as mentioned, the role of the carrier intersubband transitions is not significant in the case considered.) Optical phonons are treated as confined within the QW in accordance with the dielectric continuum model,[27] while acoustic phonons are treated as bulklike phonons. This approach is well established[31,32] and we do not go into details here. The electron collision integrals which account for the nonequilibrium optical-phonon population are determined from a solution of phonon kinetic equations (which reduce to simple rate equations in our case because of negligible optical-phonon dispersion).

Nonequilibrium optical-phonon decay into two short wavelength acoustic phonons has been taken into account and the characteristic time constant τ_d has been taken to be ≈ 8.0 ps. We did not consider the inverse process of the ''merging'' of two acoustic phonons into one optical phonon for the following reasons. In equilibrium the optical-phonon decay and creation processes caused by phonon–phonon interactions compensate each other. However, in the presence of a high electric field this balance is disturbed considerably. Due to the significant hot optical-phonon accumulation in this case, the decay processes initially dominate resulting in large acoustic-phonon populations in the QW. In fact, the acoustic phonons in heterostructures with similar elastic properties (such as GaAs/AlAs in our case) are not confined within the active region and can easily escape from the well into the surrounding AlAs matrix. (For simplicity we assume that these escaping decay phonon modes are not able to reenter the active region what usually corresponds to realistic conditions). In addition, because of the large phonon phase-space volume available near the zone boundaries, these short wavelength acoustic phonons produce small perturbations of the phonon occupation number there.[22] As a result, the bulklike decay modes do not contribute significantly to the hot-phonon buildup in the system. However, an outgoing acoustic phonon energy flux can be measured experimentally;[31] these measurements provide useful information about the transport phenomena occurring in the QW.[32]

We consider a lattice temperature, T, of 30 K. It is high enough so that it is reasonable to neglect electron gas degeneracy[23] even at low electric fields for the electron concentrations of interest in this work. The inelasticity of electron-acoustic-phonon scattering,[33] which might be significant at lower temperatures, is accurately taken into account in our model. It should be pointed out that the temperature chosen is low with respect to the LO-phonon energy for GaAs, $\hbar\omega_{\mathrm{LO}} \approx 36$ meV; therefore, at equilibrium the population of these phonons is very small and their absorption by electrons is thus a mechanism of scattering of minor importance. Hence, hot-phonon effects should be well pronounced for such conditions.

We have considered electric fields in the range 0–1000 V/cm: from very low to high enough to result in the electron escape from the quantum well. We use a right-handed orthogonal Cartesian coordinate system in which the x and y axes lie in the QW plane and the direction of the applied parallel electric field is in the negative x direction. The z axis is, of course, perpendicular to the QW plane.

A wide range of sheet (surface) 2D-electron concentrations has been considered. In this article we present our results for two different concentrations: $n_{s1} = 4.0 \times 10^{10}$ cm^{-2} and $n_{s2} = 6.4 \times 10^{11}$ cm^{-2}. As will be shown later, in the case of the lower electron concentration, n_{s1}, optical-phonon accumulation as well as the phonon reabsorption by the carriers are not significant. Therefore, the role of nonequilibrium-phonon feedback in electron transport is negligible. In other words, hot phonon and electron systems evolute almost independently in this case. For the higher electron concentration, n_{s2}, the mutual influence of the hot LO phonon and electron systems becomes strong and both the 2D-electron and confined phonon distributions display dramatic changes.

We have not taken into account electron interactions resulting from remote ionized impurities, regions of surface roughness, and electron–electron scattering. Although all these mechanisms may be important at very low temperatures and high carrier concentrations,[34,35] they should not play a crucially significant role in the range of electric fields, temperatures, and electron concentrations investigated herein.

III. MONTE CARLO SIMULATION OF NONEQUILIBRIUM OPTICAL PHONONS

The electron scattering rate by optical phonons in a QW is proportional to the square of the matrix element for the 2D-electron-optical-phonon interaction, $M^{\pm}$

$$M^{\pm} = \langle k'_x, k'_y, n'; N_q + \tfrac{1}{2} \pm \tfrac{1}{2} | H^{2\mathrm{D}} | k_x, k_y, n; N_q + \tfrac{1}{2} \mp \tfrac{1}{2} \rangle, \tag{1}$$

where $H^{2\mathrm{D}}$ stands for the 2D Fröhlich Hamiltonian of the dielectric continuum model;[27,28] N_q is the actual optical-phonon occupation number, and the quantities k_x, k_y, n and k'_x, k'_y, n' indicate initial and final electron states, respectively. The upper (lower) signs correspond to phonon emission (absorption).

In Eq. (1), the influence of nonequilibrium phonons is reflected directly by the term N_q, i.e., by the phonon occupation at the certain $\mathbf{q}_\parallel$ point in the 2D wave vector (or quasi-momentum) space. Therefore, in order to include self-consistently hot phonons in the ensemble Monte Carlo simulation, the instantaneous value of N_q should be used; as well, the carrier scattering rates must be adjusted appropriately after any optical phonon scattering event has occurred.

To account for a change in the optical-phonon population we discretized the in-plane (q_x, q_y) wave-vector space and introduced a discrete function on this mesh, N_q. The 2D mesh steps were taken as Δq_x and Δq_x. (Note that, due to the uncertainty principle, the restrictions apply to the minimum mesh step value in the $\mathbf{q}_\parallel$ space: $\min\{\Delta q_\alpha\} > 2\pi/\min\{L_\alpha\}$, where α stands for either the x or y coordinate and $\min\{L_\alpha\}$ is the smallest in-plane dimension of the QW.) In accordance with the 2D nature of confined optical phonons in QWs, after each optical-phonon emission/absorption event their population is incremented in the corresponding (q_x, q_y) cell by the value

$$\Delta N_q = \pm \left(\frac{2\pi}{\Delta q_x} \right) \left(\frac{2\pi}{\Delta q_y} \right) \left(\frac{n_s}{\mathcal{N}} \right). \tag{2}$$

Here n_s stands for the surface electron concentration in the QW, and $\mathcal{N}$ is the actual number of particles (representing 2D electrons) in the Monte Carlo simulation.

According to Eq. (2), the instantaneous value of nonequilibrium optical-phonon occupation, $N_q(t)$, can be expressed as

$$N_q(t) = N_q^{\mathrm{eq}} + \sum_i \Delta N_q^{(i)},$$

where N_q^{eq} represents the equilibrium phonon occupation number (Planck function) and the sum is taken over all optical-phonon scatterings that occurred up to the time instant t. (It also includes the phonon decay terms.) For equilibrium conditions the sum in the above expression should vanish in accordance with the principle of detailed equilibrium. When an electric field is applied, the optical-phonon population may deviate significantly from N_q^{eq} and the sum reflects these changes.

Hot optical-phonon decay into acoustic phonons was taken into account in our model by recalculating N_q for every mesh cell at the end of each time step in the Monte Carlo procedure. As mentioned previously, we have used the value of 8.0 ps for the optical-phonon decay time, τ_d.

IV. SIMULATION RESULTS

A widely used assumption in Monte Carlo simulations of carrier transport in QWs is that the optical-phonon distribution remains *in equilibrium* even if there is an electric field applied to the structure. In reality, hot electrons interacting with the phonon subsystem always drive the latter out of equilibrium. Therefore, an accurate simulation should self-consistently include *nonequilibrium optical-phonon buildup*.

The equilibrium optical-phonon occupation number, N_q^{eq}, at $T = 30$ K is very low, about 10^{-5}. Therefore, practically all generated optical phonons are nonequilibrium ones. In this article, we present our Monte Carlo calculations for two significantly different 2D electron concentrations: $n_{s1} = 4.0 \times 10^{10}$ cm^{-2} and $n_{s2} = 6.4 \times 10^{11}$ cm^{-2}. For the first

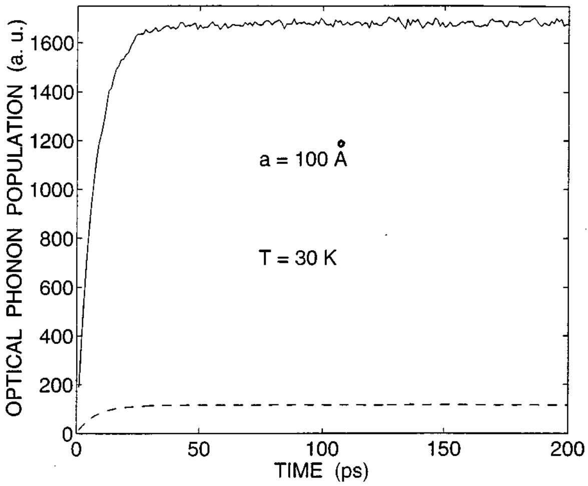

FIG. 1. Temporal evolution of the nonequilibrium optical-phonon population. GaAs quantum well: $a=100$ Å, $n_{s1}=4.0\times10^{10}$ cm^{-2} (dashed curve), $n_{s2}=6.4\times10^{11}$ cm^{-2} (solid curve); $T=30$ K, $E=200$ V/cm.

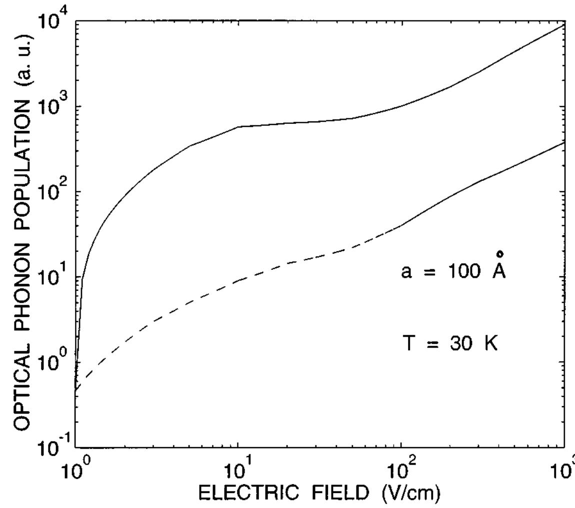

FIG. 2. Dependence of the nonequilibrium optical-phonon population on the applied electric field. GaAs quantum well: $a=100$ Å, $n_{s1}=4.0\times10^{10}$ cm^{-2} (dashed curve), $n_{s2}=6.4\times10^{11}$ cm^{-2} (solid curve); $T=30$ K.

carrier concentration, n_{s1}, the influence of hot phonons on electron transport is not important because the optical-phonon generation is insufficient even for strong electric fields. However, the situation is much different for the higher carrier concentration, n_{s2}.

The process of hot optical-phonon accumulation in GaAs QW consists of several stages. Figure 1 shows the transient response of the total nonequilibrium-phonon population, as represented by the effective lattice temperature, to an applied electric field step of 200 V/cm at $t=0$. The dashed curve corresponds to an electron concentration of 4.0×10^{10} cm^{-2} and the solid line represents the case where $n_{s2}=6.4\times10^{11}$ cm^{-2}. As seen in Fig. 1, the phonon population increases rapidly due to the rapid generation of phonons by hot 2D electrons; after 20–30 ps the population reaches saturation. The increasing part of the nonequilibrium-phonon population response is controlled by several factors. One of them is τ_e, the time necessary for an electron to approach the optical-phonon energy when the phonon emission becomes possible. At an electric field of $E=200$ V/cm, this time is approximately 8.5 ps ($\tau_e\approx\sqrt{2m^*\hbar\omega_{\mathrm{LO}}}/eE$, where e and m^* are the electron charge and the effective electron mass, respectively). Another factor is the optical-phonon decay (thermalization) time ($\tau_d\approx8.0$ ps). In fact, the generation and decay processes play the main role in the initial stage of the evolution of the nonequilibrium-phonon system. Therefore, as a result of the heating of the electron system, the phonon population starts to grow almost linearly with time. On the other hand, together with the accumulation and decay mechanisms considered, the rate of hot optical-phonon reabsorption by electrons increases as well because it is linearly proportional to the phonon occupation number, N_q; see Eq. (1). The latter process becomes important for significant nonequilibrium-phonon populations, i.e., during the final stages of the hot optical-phonon population evolution and is more pronounced in the case of high carrier concentrations, as would be expected. The counterplay of the phonon emission and decay as well as the induced reabsorption of phonons by 2D carriers control the steady-state value of the hot LO-phonon population.

Figure 2 shows the total (integral) nonequilibrium LO-phonon population plotted versus the applied electric field intensity for electron concentrations of 4.0×10^{10} cm^{-2} (dashed curve) and 6.4×10^{11} cm^{-2} (solid curve). According to this figure, over a wide range of electric field, 100 V/cm $<E<$ 1000 V/cm, the hot optical-phonon population grows near *linearly* with increasing electric field. On the other hand, at low fields the dependence considered is nonlinear. The explanation of this fact is the following. At electric fields lower than 10–20 V/cm electron transport in the QW is controlled primarily by *bulklike acoustic phonon* scattering. This scattering mechanism efficiently prevents the carriers from approaching the optical-phonon emission threshold; therefore, such phonon accumulation in the structure is weak and is caused only by the high-energy tail of the electron distribution. Increasing the electric field results in the heating of the electron subsystem causing electron runaway from acoustic phonon scattering as well as in exponentially enhanced optical-phonon emission. The counterplay of acoustic and optical-phonon scattering, when the latter mechanism becomes more and more dominant with increasing field, leads to the nonlinear dependence in Fig. 2 at $E<15$ V/cm.

For moderate fields of 100 V/cm $<E<$ 500 V/cm, optical-phonon emission is much stronger than acoustic-phonon scattering; it controls the carrier mobility *stabilizing* effectively further electron energy growth in this region. It should be emphasized that in the case of such electric fields, electron motion in the QW structure corresponds to the so-called *streaming regime*.[33,36–38] Electrons accelerate until they acquire the energy of the optical phonon. Then they rapidly emit these phonons and are scattered down to the bottom of the energy subband. This process repeats periodically in time. Because the emission rates at energies just above the optical-phonon energy are very high, electrons cannot penetrate much above this energy threshold. Based on

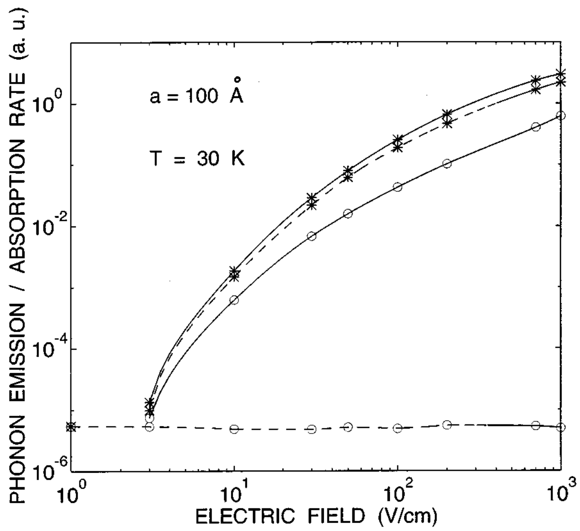

FIG. 3. Optical-phonon emission/absorption rate vs the applied electric field. Solid curves illustrate the phonon emission intensity, dashed ones, the absorption. Empty circles denote the case when nonequilibrium LO phonons are neglected; stars correspond to the self-consistent simulation which takes into account hot phonons. GaAs quantum well: $a=100$ Å; $T=30$ K.

these considerations, in the streaming regime the electron drift velocity saturates at the value

$$v_s=\sqrt{\frac{\hbar\omega_{\rm LO}}{2m^*}}. \tag{3}$$

Note that, if electric field is low, less than 10–20 V/cm, the frequency of periodic electron motion in quasi-momentum space is comparable with the rate of the carrier scattering by acoustic phonons. As a result, the streaming motion does not occur in this case because electrons are prevented from acquiring significant energies. On the other hand, at electric fields above 400–500 V/cm, electrons start *running away* from optical-phonon scattering and periodic carrier motion does not occur either.

As mentioned previously, at moderate electric fields the total joule power pumped into the electron system by the external electric field is dissipated mostly via the intensive emission of LO phonons in the streaming mode. This power, $P_J= env_sE$, for the saturated electron drift velocity of Eq. (3) is a *linear function* of the electric field. Therefore, the total nonequilibrium optical-phonon population, which is proportional to P_J, is also a *linear function* of E in the moderate field range; see Fig. 2.

As illustrated by the above considerations, the roles of the different electron-phonon scattering mechanisms depend on the applied electric field intensity. The presence of pronounced hot optical-phonon accumulation may also modify dramatically these rates strongly affecting all transport properties in the QW. Figure 3 illustrates the influence of nonequilibrium phonons on 2D-electron scattering in the system by LO phonons. As discussed previously, the latter process makes the dominant contribution to the electron energy dissipation in QWs in the moderate-to-high electric field range.

When the buildup of hot phonons is negligible, as in the case of a low concentration 2D-electron gas (the curves with empty circles in Fig. 3), optical phonon absorption by carriers remains small and almost constant for electric field range under consideration (the dashed curve with empty circles.) In this case, such an absorption rate is controlled by the negligible equilibrium LO-phonon population corresponding to a 30 K lattice temperature. (As mentioned above, the equilibrium occupation number, N_q, is 10^{-5} of the order of magnitude in this case). Note that for small disturbances of the phonon system, the much larger emission rate (the solid curve with empty circles in Fig. 3) is due to spontaneous phonon emission with a relative weight N_q+1. At higher fields, owing to a significant electron heating in the QW, LO-phonon emission increases by several orders of magnitude as the electric field increases up to 1000 V/cm. However, a sufficient part of the power pumped by hot-electron gas to the confined hot optical-phonon subsystem leaves the structure by means of significant strongly nonequilibrium bulklike acoustic-phonon radiation. As mentioned, the latter phonons are produced as a result of the hot optical phonon decay.[21,39]

In the case of high carrier concentrations represented by the curves with stars in Fig. 3, when nonequilibrium-phonon accumulation is pronounced, the optical-phonon absorption intensity increases dramatically in contrast to the previously discussed case; compare the two dashed curves in Fig. 3. The rate of the latter scattering mechanism becomes even closer to that of the corresponding LO-phonon emission in the case considered—the solid curve with stars. Such behavior is in accordance with Eq. (1) when N_q is comparable to or larger than unity.

Due to the substantially enhanced optical-phonon absorption rate in the case of very pronounced hot LO-phonon accumulation, the energy stored in the confined nonequilibrium-phonon system does not leave the QW structure. This energy is efficiently transferred back to the electron subsystem by means of hot-phonon reabsorption. In turn, the additional energy gained by the carriers leads to further enhancement of the optical phonon emission in the system and so on. Such a ‘‘positive feedback’’ between the electron and phonon subsystems causes a dramatic increase in the optical-phonon emission rate (the solid curve with stars in Fig. 3) in comparison with that for negligible hot-phonon accumulation in the QW (the solid curve with empty circles in Fig. 3). The optical-phonon emission/absorption rates in the case of high electron concentration (the curves with stars) change in the same way responding to the changes of the applied electric field intensity. This indicates that there is a certain quasi-steady-state established between the carrier and the phonon subsystems in the QW.

The changes in the mutual interaction and the strength of coupling between the hot electron and nonequilibrium optical-phonon systems are reflected by their distributions in the structure under consideration. Figures 4 and 5 show the phonon distribution functions at $E=200$ V/cm and $T=30$ K for the two different electron sheet concentrations of 4.0 $\times10^{10}$ cm^{-2} and 6.4$\times10^{11}$ cm^{-2}, respectively. The first fig-

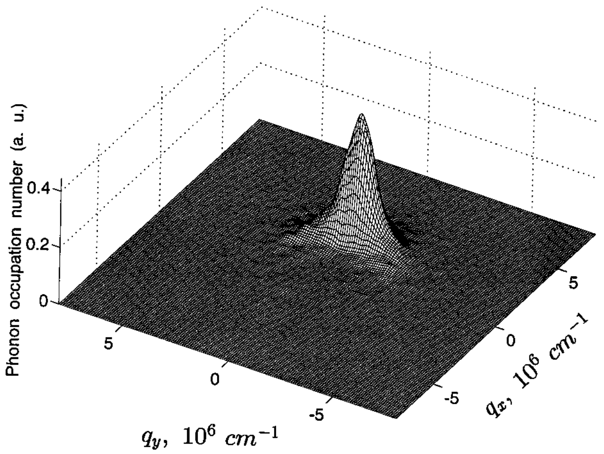

FIG. 4. Nonequilibrium optical-phonon distribution function. The simulation self-consistently includes nonequilibrium optical phonons. GaAs quantum well: $a=100$ Å, $n_{s1}=4.0\times 10^{10}$ cm^{-2}; $T=30$ K, $E=200$ V/cm.

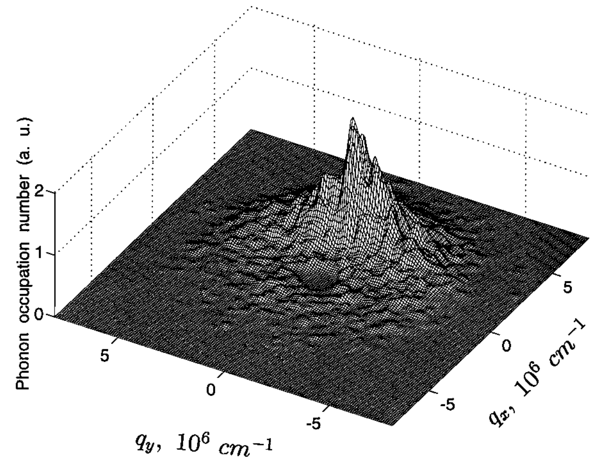

FIG. 5. Nonequilibrium optical-phonon distribution function. The simulation self-consistently includes nonequilibrium optical phonons. GaAs quantum well: $a=100$ Å, $n_{s2}=6.4\times 10^{11}$ cm^{-2}; $T=30$ K, $E=200$ V/cm.

ure demonstrates a smooth symmetrical phonon distribution in the two-dimensional wave vector space (q_x, q_y) for the case of the lower electron concentration. For $n_{s1}=4.0\times 10^{10}$ cm^{-2} the mutual influence of the electron and phonon systems is not significant. Periodic oscillation of electrons in the quasi-momentum space (streaming) results in significant generation of optical phonons only in certain regions of the phonon quasi-momentum space. This function has a maximum at the wave-vector $\mathbf{q}_\| = (q_{\max}, 0)$, where $q_{\max} = \sqrt{2m^*\omega_{\mathrm{LO}}/\hbar}$, and it is equal to the equilibrium population, $1/(\exp(\hbar\omega_{\mathrm{LO}}/T)-1)$, at the origin, $\mathbf{q}_\|=0$, due to restrictions imposed by energy and quasi-momentum conservation on electron-optical-phonon scattering.

The hot LO-phonon distribution is symmetrical with respect to the q_x-axis (the direction of the electric field) and is shifted in the x direction. As we will see later (Figs. 6 and 7), the phonon distribution displays the analogous features of the electron distribution. Optical phonons with positive q_x wave-vector components prevail over those with negative components; therefore, the nonequilibrium-phonon subsystem preserves a certain directed momentum and energy (in the direction opposite to the electric field due to the negative electron charge) which might be transferred back to the 2D-carrier system.

In Fig. 4 there is a circular region near the coordinate origin, $\mathbf{q}_\|=0$, where the optical-phonon population remains unchanged, i.e., it is equilibrium. According to the conservation laws for optical-phonon scattering, the shortest and the longest possible emitted/absorbed phonon wave-vector $\mathbf{q}$ magnitudes are defined by the following equations:

$$q_{\min} = |\mp k \pm k'| = \frac{\sqrt{2m^*}}{\hbar} |\mp \sqrt{\epsilon} \pm \sqrt{\epsilon \pm \hbar\omega_{\mathrm{LO}}}|, \tag{4}$$

$$q_{\max} = |k + k'| = \frac{\sqrt{2m^*}}{\hbar} |\sqrt{\epsilon} + \sqrt{\epsilon \pm \hbar\omega_{\mathrm{LO}}}|, \tag{4}$$

where k and k' indicate the magnitudes of initial and final electron state wave numbers, respectively, and ϵ is electron energy before the scattering. The upper (lower) signs in the above expression stand for phonon absorption (emission). As the electron energy increases the minimum phonon wave vector becomes shorter and the maximum magnitude of $\mathbf{q}$ increases as indicated by Eqs. (4).

The nonequilibrium LO-phonon distribution in Fig. 5 corresponds to the case where $n_{s2}=6.4\times 10^{11}$ cm^{-2}. Referring to Figs. 4 and 5, one can see that if the 2D-electron concentration increases by a factor of 16, i.e., it becomes equal to 6.4×10^{11} cm^{-2}, the hot optical-phonon population is larger that unity, and stimulated phonon absorption by the 2D electrons is likely to occur. Such reabsorption may substantially randomize the phase of the carrier coherent streaming motion in the quasi-momentum space.[1] This broadens the carrier distribution, washes out the kink at optical-phonon emission threshold, and leads to a more isotropic distribution. On the other hand, the heated electrons with those more symmetric distribution functions emit optical phonons with more arbitrarily oriented wave vectors (see Fig. 5). In turn, as these phonons are reabsorbed by electrons they transform the carrier distribution functions so that the latter have even more symmetric forms, and so on. The above reasoning shows that the transition from *low* electron concentrations—when phonon absorption almost has little affect on electron transport—to *high* electron concentrations—when this influence becomes significant—is dramatic; this transition completely transforms the carrier and phonon distribution functions as is evident upon comparison of Figs. 4 and 5.

For higher electron concentration, n_{s2}, when nonequilibrium-phonon reabsorption is significant (Fig. 5), the optical-phonon distribution in the $\mathbf{q}_\|$-vector space is substantially wider than in the case of low electron concentration. However, it has a larger magnitude than that in Fig. 4 because more electrons create more phonons; in the case of significant hot-phonon buildup, the electron-optical-phonon interaction smears out the 2D-electron distribution and almost completely destroys the forward-peaked anisotropy of the nonequilibrium-phonon distribution; the latter becomes nearly isotropic. Therefore, the 2D electrons do not gain any prevailing directed momenta as a result of reabsorbing such

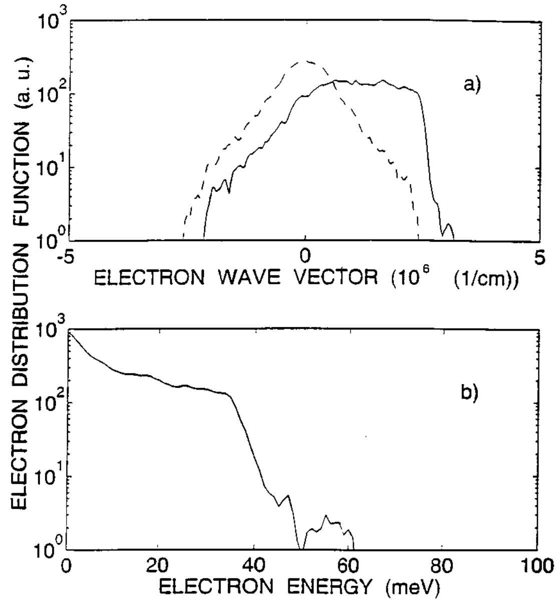

FIG. 6. (a) A 2D-electron distribution function averaged over k_y as a function of k_x (solid curve) and averaged over k_x as a function of k_y (dashed curve); (b) A 2D-electron distribution function as a function of electron energy. Nonequilibrium optical phonons are neglected; GaAs quantum well: $a=100$ Å, $n_{s1}=4.0\times10^{10}$ cm^{-2}, $E=200$ V/cm, $T=30$ K; the field is antiparallel to the k_x axis.

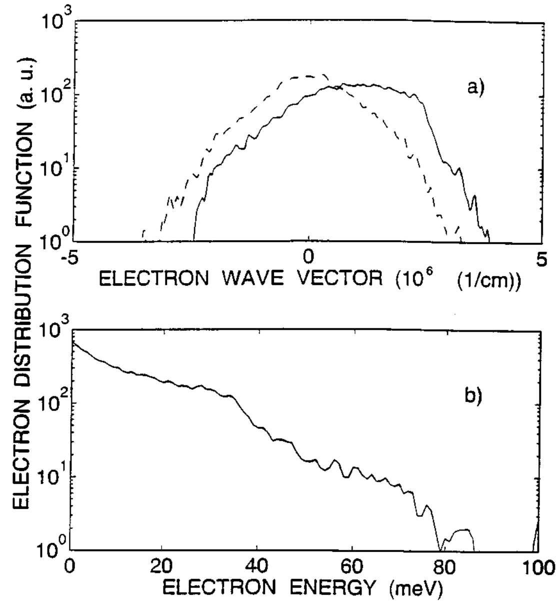

FIG. 7. (a) A 2D-electron distribution function averaged over k_y as a function of k_x (solid curve), averaged over k_x as a function of k_y (dashed curve); (b) the distribution function as a function of electron energy. Hot optical phonons are taken into account; GaAs quantum well: $a=100$ Å, $n_{s2}=6.4\times10^{11}$ cm^{-2}, $E=200$ V/cm, $T=30$ K; the field is antiparallel to the k_x axis.

phonons. This interaction does, however, lead to an increase in the carrier mean energy.

Note that for high electron concentration, the radius of the circle of prohibited phonon wave numbers near the coordinate origin, $\mathbf{q}_{\parallel}=0$, becomes smaller (see Fig. 5), indicating an increase in the energy of the scattering participating carriers according to Eqs. (4).

As Figs. 4 and 5 show, hot LO-phonon distributions differ significantly in the cases of the lower and the higher electron concentrations. Naturally, due to a strong coupling between the confined carrier and optical-phonon systems in the structure, the carrier distributions also vary in these two cases.

Figures 6 and 7 illustrate the influence of hot optical-phonon reabsorption on the 2D-electron distribution function in the case of the higher electron concentration, $n_{s2}=6.4\times10^{11}$ cm^{-2}. Figure 6 corresponds to the Monte Carlo simulation with an equilibrium optical-phonon distribution function while Fig. 7 is obtained from the self-consistent solution of the kinetic equations for electrons and phonons. It should be mentioned that for the case of the lower carrier concentration, $n_{s1}=4.0\times10^{10}$ cm^{-2}, the results related to electrons and found by the self-consistent approach are identical to those obtained using the model equilibrium optical phonons. The solid curves in Figs. 6(a) and 7(a) illustrate the dependence of the electron distribution function on the electron in-plane wave vector component k_x, i.e., the function is averaged over k_y. The dashed curves represent the electron distribution function versus k_y (the average over k_x). The energy dependence of the 2D-electron distribution function is also shown in Figs. 6(b) and 7(b).

In the case when hot phonons are neglected in the simulation, the 2D-electron distribution in the QW structure displays the features related to the streaming regime of the carrier motion. The distribution is shifted against the electric field (i.e., in the positive k_x direction) in the electron wave-vector space [the solid curve in Fig. 6(a)] and it also retains an axial symmetry in this direction as illustrated by the dashed curve in Fig. 6(a). The distribution function dependence on electron energy [the graph in Fig. 6(b)] exhibits a well pronounced kink at carrier energies close to the optical-phonon energy (≈36 meV).

As Fig. 6 indicates, there is a significant population of the ''slow'' carriers near the origin, $\mathbf{k}_{\parallel}=0$, in the case when hot-phonon feedback to electrons is not taken into account. In accordance with the streaming mechanism, at moderate electric fields (e.g., 200 V/cm as in the case presented in this figure) electrons gain their energy slowly until they reach the optical-phonon energy. Then they very rapidly emit optical phonons and are scattered back to the bottom of the energetic subband. Therefore, the carriers spend a significant fraction of time in the region near $\mathbf{k}_{\parallel}=0$. Acoustic-phonon scattering, which is dominant at low electron energies, efficiently ''slows down'' the electrons and contributes to the effect considered.

Comparing Figs. 6 and 7 we can see how dramatically the electron distribution is affected by the induced nonequilibrium optical-phonon reabsorption. The carrier distribution function smears out, its forward-peaked anisotropy is reduced, and it becomes more symmetric in the $\mathbf{k}_{\parallel}$ space; the mean electron energy increases and a steep kink at the optical-phonon energy disappears, indicating an increase in the population of the high-energy electrons. This shows that the quasi-periodic electron motion in the momentum space is almost completely destroyed as a result of the phonon system

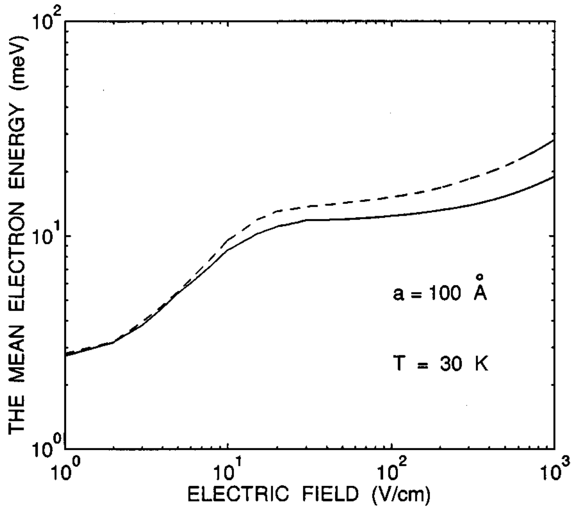

FIG. 8. Dependence of the mean electron energy on the applied electric field for the cases when nonequilibrium optical phonons are neglected (solid curve) and taken into account (dashed curve). GaAs quantum well: $a = 100$ Å, $n_{s2} = 6.4 \times 10^{11}$ cm^{-2}; $T = 30$ K.

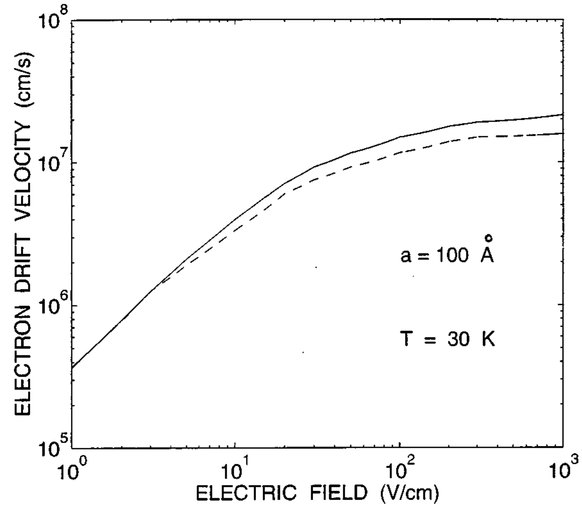

FIG. 9. Dependence of the electron drift velocity on applied electric field for the cases when nonequilibrium optical phonons are neglected (solid curve) and taken into account (dashed curve). GaAs quantum well: $a = 100$ Å, $n_{s2} = 6.4 \times 10^{11}$ cm^{-2}; $T = 30$ K.

action. Therefore, on average, the 2D-electron mean energy increases in this case while carrier drift velocity decreases.

As shown, changes in the 2D-electron distribution function, caused by hot-phonon feedback, modify the integral carrier characteristics such as the drift velocity and the mean energy. The hot-phonon effects considered herein are very pronounced for high electron concentrations and strong electric fields. Figure 8 demonstrates the influence of nonequilibrium optical phonons on the mean electron energy; the dashed curve corresponds to the case of the higher electron concentration, n_{s2}, when hot-phonon effects are pronounced, while the solid curve represents the case of an almost undisturbed phonon distribution. Here, particular cases, such as shown above in Fig. 6, are summarized. The calculations have been carried out for a 30 K lattice temperature and for the electric field interval of 1–1000 V/cm and.

In analyzing Fig. 8 it is useful to consider three characteristic regions of the electric field. At fields less than 10–15 V/cm, all the carrier energy gained from the electric field is dissipated via acoustic-phonon emission. In this region the electron mean energy starts to grow nearly quadratically with increasing electric field; however, slightly above 4–5 V/cm the dependence evolves into a square-root dependence indicating a significant heating of 2D electrons. Saturation at very low fields in the first characteristic region ($E < 1$ V/cm) is due to the lower limit imposed by the thermal electron energy which is about 2.6 meV for a 30 K lattice temperature. As discussed previously, in the moderate field region, $15\ \text{V/cm} < E < 300\ \text{V/cm}$, a significant part of the electron energy is transferred to confined optical phonons. The LO-phonon emission, which becomes the dominant scattering mechanism in the QW system, stabilizes the mean electron energy at approximately 12.0 meV in this field region. Electrons start to run away from optical-phonon scattering for electric fields above 400–500 V/cm. With the induced hot optical-phonon reabsorption taken into account (the dashed curve in Fig. 8), the electron subsystem dissipates its energy at slower rate; this can be seen by comparing Figs. 6 and 7. Consequently, due to the additional energy absorbed back by electrons, the carrier runaway starts at lower electric fields in this case.

The influence of nonequilibrium optical phonons on the carrier drift velocity in the field range 1–1000 V/cm is shown in Fig. 9. The solid curve corresponds to the case when hot phonons are neglected and the dashed curve illustrates the results when these phonons are taken into account. In accordance with the streaminglike nature of electron motion at moderate electric fields ($100\ \text{V/cm} < E < 1000\ \text{V/cm}$) in the case of negligible nonequilibrium-phonon buildup, the electron drift velocity (the solid curve) should saturate at the value of v_s given by Eq. (3). Using the parameters for GaAs, we get $v_s \approx 2.15 \times 10^7$ cm/s, which is in good agreement with the graph.

In the case of pronounced hot-phonon buildup (the dashed curve in Fig. 9), the electron drift velocity is approximately 1.5 times smaller than in the former case of near-equilibrium optical phonons in the QW system (the solid curve).

As Figs. 4, 5, 8, and 9 illustrate for the electric fields investigated in this work, nonequilibrium optical phonons lead to significant randomization of the directed electron quasi-momentum and to diffusivelike carrier heating in the system. The 2D-electron distribution spreads out intensively in the wave-vector space and loses a significant part of its field-directed anisotropy. Because the electron and the LO-phonon systems are strongly coupled in this case, similar changes are displayed by the hot-phonon distribution as well; Figs. 4 and 5 illustrate this clearly.

V. CONCLUSIONS

We have employed Monte Carlo simulation techniques to solve self-consistently the coupled kinetic equations for electrons and optical phonons confined in a GaAs quantum well. We have investigated the effect of nonequilibrium optical phonons on electron transport at a lattice temperature of 30 K.

We have found that for the range of electric fields of 10–1000 V/cm the nonequilibrium optical-phonon population in 2D GaAs/AlAs QW structures grows nearly *linearly* with increasing electric field intensity.

For the case of low 2D-electron concentrations in the QW, the hot optical-phonon distribution reflects the dominant features of the electron distribution from which it originated. Thus, on average, the nonequilibrium-phonon system preserves a certain directed quasi-momentum in the opposite direction to that of electric field. However, the feedback of the optical-phonon distribution function on the electrons is not essential: both the electron and phonon systems are almost independent in this case.

For high electron concentrations, enhanced hot-phonon emission and reabsorption lead to a nonequilibrium-phonon distribution which intensively spreads out in the quasi-momentum space and its forward-peaked anisotropy is reduced greatly. As a result of interactions with the 2D electrons, the phonon subsystem behaves more like an *isotropic distribution*. The influence of such a smeared out, nearly isotropic hot optical-phonon distribution on electron transport in the QW is reflected by an increase of high-energy electron population and a decrease of the carrier drift velocity as manifested by an increase in the mean electron energy or the electron subsystem temperature.

It should be pointed out that, even though the nonequilibrium LO phonon as well as the electron distributions exhibit dramatic changes due to electron-hot-phonon interactions, the integral 2D-electron characteristics—such as the drift velocity and the mean energy—remain relatively unperturbed in the electric field and electron concentration ranges presented herein. However, with increasing electron concentration, nonequilibrium-phonon effects become increasingly pronounced.

ACKNOWLEDGMENTS

The authors would like to express their gratitude to Dr. M. A. Stroscio for helpful discussions, useful remarks, and critical reading of the manuscript. This work was supported by the U.S. Army Research Office.

[1] W. Cai, M. C. Marchetti, and M. Lax, Phys. Rev. B **37**, 2636 (1988).
[2] M. Rieger, P. Kocevar, P. Lugli, P. Bordone, L. Regianni, and S. M. Goodnick, Phys. Rev. B **39**, 7866 (1989).
[3] J. Shah, R. C. C. Leite, and J. F. Scott, Solid State Commun. **8**, 1089 (1970).
[4] D. Y. Oberli, G. Böhm, and G. Weimann, Phys. Rev. B **47**, 7630 (1993).
[5] K. T. Tsen, R. P. Joshi, D. K. Ferry, A. Botchkarev, B. Sverdlov, A. Salvador, and H. Morkoc, Appl. Phys. Lett. **68**, 2990 (1996).
[6] E. D. Grann, K. T. Tsen, and D. K. Ferry, Phys. Rev. B **53**, 9847 (1996).
[7] R. Mickevičius, V. Mitin, G. Paulavičius, V. Kochelap, M. A. Stroscio, and G. J. Iafrate, J. Appl. Phys. **80**, 5145 (1996).
[8] V. V. Mitin, G. Paulavičius, and N. A. Bannov, Superlattices Microstruct. (accepted).
[9] S. Koch and T. Mizutani, IEEE Trans. Electron Devices **41**, 1498 (1994).
[10] K. Kurishima, H. Nakajima, T. Kobayashi, Y. Matsuoka, and T. Ishibashi, IEEE Trans. Electron Devices **41**, 1319 (1994).
[11] R. Kuburz, J. Schmid, and R. Popovich, IEEE Trans. Electron Devices **41**, 315 (1994).
[12] J. Faist, F. Capasso, D. Sivko, C. Sirtori, A. Hutchhinson, and A. Cho, Science **264**, 553 (1994).
[13] V. F. Elesin and Yu. V. Kopaev, Solid State Commun. **96**, 897 (1995).
[14] P. J. Price, Physica B **134**, 164 (1985).
[15] P. Kocevar, Physica B **134**, 155 (1985).
[16] T. Ruf, K. Wald, P. Yu, K. Tsen, H. Morcoč, and K. Chan, Superlattices Microstruct. **13**, 203 (1993).
[17] R. Mickevičius and A. Reklaitis, J. Phys.: Condens. Matter **2**, 7883 (1990).
[18] K. Leo, W. Rühle, and K. Ploog, Solid-State Electron. **32**, 1863 (1989).
[19] P. Blockmann, J. Young, P. Hawrylak, and H. M. van Driel, Semicond. Sci. Technol. **9**, 746 (1994).
[20] K. Santra and C. Sarkar, Phys. Rev. B **47**, 3598 (1993).
[21] F. Vallee and F. Bogani, Phys. Rev. B **43**, 12 049 (1991).
[22] K. Kim, K. Hess, and F. Capasso, Appl. Phys. Lett. **52**, 1167 (1988).
[23] P. Lugli and D. K. Ferry, IEEE Trans. Electron Devices **32**, 2431 (1985).
[24] S. M. Goodnick and P. Lugli, Phys. Rev. B **37**, 2578 (1988).
[25] R. Mickevičius and A. Reklaitis, Solid State Commun. **64**, 1305 (1987).
[26] N. S. Mansour, Y. M. Sirenko, K. W. Kim, M. A. Littlejohn, J. Wang, and J. P. Leburton, Appl. Phys. Lett. **67**, 3480 (1995).
[27] N. Mori and T. Ando, Phys. Rev. B **40**, 6175 (1989).
[28] K. W. Kim, M. A. Stroscio, A. Bhatt, R. Mickevicius, and V. V. Mitin, J. Appl. Phys. **70**, 319 (1991).
[29] R. Mickevičius, V. V. Mitin, K. W. Kim, M. A. Stroscio, and G. J. Iafrate, J. Phys.: Condens. Matter **4**, 4959 (1992).
[30] G. Fasol, M. Tanaka, H. Sakaki, and Y. Horikosh, Phys. Rev. B **38**, 6056 (1988).
[31] P. Hawker, A. Kent, O. Hughes, and L. Challis, Semicond. Sci. Technol. **7**, 29 (1992).
[32] V. V. Mitin, G. Paulavičius, N. Bannov, and M. A. Stroscio, J. Appl. Phys. **79**, 8955 (1996).
[33] R. Mickevičius, V. Mitin, U. K. Harithsa, D. Jovanovic, and J. P. Leburton, J. Appl. Phys. **75**, 973 (1994).
[34] J. P. G. Taylor, K. J. Hugill, D. D. Vvedensky, and A. MacKinnon, Phys. Rev. Lett. **67**, 2359 (1991).
[35] J. A. Nixon and J. H. Davies, Phys. Rev. B **41**, 7929 (1990).
[36] W. Shockley, Bell Syst. Tech. J. **30**, 990 (1951).
[37] S. Komiyama, Adv. Phys. **31**, 255 (1982).
[38] D. Jovanovic and J. P. Leburton, Superlattices Microstruct. **11**, 141 (1992).
[39] K. Kral, Phys. Status Solidi B **174**, 209 (1992).